PHYSICAL REVIEW D **86,** 113016 (2012)

Search for new physics with neutrinos at radioactive ion beam facilities

Catalina Espinoza,[1,2,*] Rimantas Lazauskas,[3,†] and Cristina Volpe[4,‡]

[1]*Centro de Física Teórica de Partículas, Instituto Superior Técnico, Universidade Técnica de Lisboa, Avenida Rovisco Pais 1, 1049-001 Lisboa, Portugal*

[2]*Departamento de Física Teórica and IFIC, Universidad de Valencia-CSIC, E-46100 Valencia, Spain*

[3]*IPHC, IN2P3-CNRS/Université Louis-Pasteur BP 28, F-67037 Strasbourg cedex 2, France*

[4]*AstroParticule et Cosmologie (APC), Université Paris Diderot—Paris 7, 10, rue Alice Domon et Léonie Duquet, 75205 Paris cedex 13, France*

(Received 29 February 2012; published 27 December 2012)

We propose applications of radioactive ion beam facilities to investigate physics beyond the Standard Model. In particular, we focus upon the search for sterile neutrinos and the possible measurement of coherent neutrino-nucleus scattering, by means of a low-energy beta beam with a Lorentz boost factor $\gamma \approx 1$. In both cases, we consider ^{8}Li and ^{8}B ions as neutrino sources. In the considered setup, the collected radioactive ions are sent inside a 4π detector. For the first application, we provide the number of events associated with neutrino-nucleus coherent scattering, when the detector is filled with a noble liquid. For the sterile search, we consider that the spherical detector is filled with a liquid scintillator, and that the neutrino detection channel is inverse beta decay. We provide the exclusion curves for the sterile neutrino mixing parameters, based upon the 3 + 1 formalism, depending upon the achievable ion intensity. Our results are obtained both from total rates, and by including spectral information with binning in energy and in distance. The proposed experiment represents a possible alternative to clarify the current anomalies observed in neutrino experiments.

DOI: 10.1103/PhysRevD.86.113016 PACS numbers: 14.60.St, 13.15.+g, 29.38.−c, 23.40.−s

I. INTRODUCTION

A wealth of experimental results on neutrino oscillations have been gathered since the neutrino oscillation discovery. Currently most of the data from accelerators, reactors, and the Sun are interpreted within the theoretical framework of three active neutrino flavors, involving the Maki-Nakagawa-Sakata-Pontecorvo matrix relating the flavor to the mass basis. In this case, the number of unknown parameters is limited to three angles and three (one Dirac and two Majorana) phases, most of which have been determined. Recently, the T2K Collaboration has found an indication of a nonzero value for the still-unknown neutrino mixing angle θ_{13}, at 2.5σ [1]. A nonzero θ_{13} is also consistent with the first Double-Chooz results [2]. New results on the third neutrino mixing angle have recently been obtained by the Daya-Bay [3] and RENO [4] collaborations. The most precise measurement is currently $\sin^2 2\theta_{13} = 0.092 \pm 0.016(\text{stat}) \pm 0.005(\text{syst})$ at 5.2σ from Daya-Bay [3]. Note that a combined analysis had previously favoured a nonzero θ_{13} (see, e.g., Refs. [5,6]). Beyond the intrinsic theoretical interest of knowing the last mixing angle value, its determination is a key step for setting up a strategy to search for leptonic *CP* violation. With an upgrade of the T2K and NOνA accelerator experiments, a (small) fraction of the Dirac δ values can be explored [7]. The coverage of most of the Dirac phase values can be attained only with next-generation experiments including superbeams or beta beams (see, e.g., Ref. [8]). The DAEDALUS project constitutes an interesting alternative [9]. Other open questions concerning fundamental neutrino properties include the neutrino mass scale, for which the KATRIN experiment should deliver results in the coming years [10], the neutrino mass hierarchy, the Majorana versus Dirac nature of neutrinos, and the possible existence of sterile neutrinos.

Besides the essential information gathered from terrestrial experiments, neutrino properties have an important impact on astrophysical and cosmological observations. Numerous examples exist in the literature showing that information can be extracted based on unknown neutrino properties, or discussing their implications on a variety of phenomena, like for example (stellar and primordial) nucleosynthesis processes. Recently it has been shown, e.g., that a nonzero *CP*-violating Dirac phase might have an impact in core-collapse supernovae [11,12], or on big bang nucleosynthesis [13]. Numerous studies have investigated the effects of sterile neutrinos, e.g., on the *r* process (such as Ref. [14]) or on the primordial light-element abundances, like in Ref. [15]. Recent cosmological constraints on sterile neutrinos can be found in Ref. [16].

While neutrino oscillations are nowadays an established fact, several anomalies have recently been observed that cannot be explained within the standard three-active-neutrino framework. First, the MiniBooNE antineutrino and neutrino oscillation results are not fully understood, while an increased statistics should help to elucidate the

*m.catalina@cftp.ist.utl.pt
†Rimantas.Lazauskas@IReS.in2p3.fr
‡volpe@ipno.in2p3.fr

low-energy excess and the oscillation hypothesis [17]. This experiment, which was supposed to confirm/rule out LSND, has found an indication of neutrino oscillations at a Δm^2 of about 1 eV^2 both in the antineutrino channel, using decay-at-rest muons [18], and the neutrino channel, based upon decay-in-flight pions [19]. Note that the KARMEN experiment, employing a similar neutrino source and detector, has found no indication of oscillations and has excluded most of the LSND oscillation parameter region [20]. The second anomaly is known as the "reactor anomaly" [21]. Indeed, a recent reevaluation of the electron antineutrino flux from reactors has shown a shift in the flux renormalization by 3% [22] compared to the previous predictions. The reanalysis of the reactor experiments, using this new flux, has shown a significant inconsistency with the three-neutrino oscillation hypothesis. Finally, some years ago, the GALLEX and SAGE experiments pointed out an anomaly in the neutrino flux measured by putting intense static ^{37}Ar and ^{51}Cr sources inside their detectors. This is referred to as the gallium anomaly. Reference [23] has performed a detailed analysis including the 5%–10% uncertainty on the corresponding neutrino-nucleus cross sections, showing that the gallium anomaly's statistical significance is at the level of 3σ.

Currently the ensemble of the accelerator, reactor, and gallium anomalies is the object of debate and has triggered an intense investigation. The possible interpretations exploit, for example, one or more sterile neutrinos, such as in Ref. [24], or a combination of sterile neutrinos with nonstandard interactions, like in Ref. [25], while none of the proposed explanations so far provides a comprehensive understanding of all the data. Numerous proposals are being put forward to confirm/rule out possibilities [26–30]. Among these, Ref. [26] proposes to put intense radioactive sources inside neutrino detectors, while Ref. [31] has pointed out the possibility of using intense ion sources produced at nuclear facilities. It is clear that independent and aimed experiments are necessary to clarify the present situation.

Reference [32] has proposed the idea of establishing a low-energy beta beam[1] facility to dispose of neutrino beams in the 100 MeV energy range, based upon the beta decay of radioactive ions, with $\gamma \approx 1$ (γ being the Lorentz factor) or with an ion boost γ of 2 to 7 (typically).[2] In the first case, the neutrino fluxes are those of ions that decay at rest, while in the second case, beams of variable average energy are obtained through a boost of the ions. The advantage of having such a facility is to dispose of pure (in flavor) and well-known electron neutrino (or antineutrino) fluxes. The physical applications cover neutrino-nucleus interaction and fundamental interactions studies, oscillation searches, and core-collapse supernova physics, as pointed out in Ref. [32] (for a review, see Ref. [8]). These issues have been investigated in detail in a series of works, including neutrino-nucleus interaction aspects in Refs. [36–39], a measurement of the neutrino magnetic moment in Ref. [40], a test of the Conserved Vector Current hypothesis in Ref. [41], a measurement of the Weinberg angle at low momentum transfer in Ref. [42], the search for non-standard interactions in Ref. [43] and a measurement of coherent neutrino-nucleus scattering in Ref. [44], the oscillation towards sterile in Ref. [45], and an interpolation method to extract the neutrino fluxes from supernovae in Ref. [46]. In Ref. [47], the connection between neutrino-nucleus interaction and double beta decay is pointed out in relation with a low-energy beta beam. Most of these applications are based on stored boosted ions. In Ref. [40], we have considered the configuration with $\gamma \approx 1$, with radioactive ions sent to a target inside a 4π detector in search of the neutrino magnetic moment. Note that Ref. [31] has taken the same configuration for a sterile neutrino search.

In this paper, we consider a low-energy beta beam with $\gamma \approx 1$. We consider that the ions are injected into a target inside a 4π detector. The purpose is to use the resulting very low-energy neutrino flux to search for new physics. Here we explore two applications: the search for sterile neutrinos and a coherent neutrino-nucleus scattering measurement. We show that, depending on the ion intensity, a coherent neutrino-nucleus scattering measurement could be performed. Then, we focus on the search for one sterile neutrino in a 3 + 1 neutrino-flavor framework and present exclusion plots for the sterile neutrino mixing parameters. The manuscript is structured as follows: We present our framework in Sec. II, while our numerical results are given in Sec. III. Section IV is a conclusion.

II. GENERAL FRAMEWORK

A. Possible setups and corresponding neutrino fluxes

Radioactive ion beam facilities produce intense radioactive ions decaying through beta decay or electron capture. Since specific radioactive ions can be selected, a pure electron (anti)neutrino flux can be obtained. As first proposed in Ref. [32], there exist two alternative ways to produce low-energy neutrinos (Fig. 1). In the first scenario, the decaying ions are stored inside a storage ring, while the emitted (anti)neutrinos are detected in a detector located close to the storage ring. If the stored ions are boosted, the corresponding neutrino spectra have variable energy with the average energy given by $\langle E_\nu \rangle \approx \gamma Q/2$, with Q being the Q value of the beta-decaying nucleus. Depending on the application envisaged, the neutrino fluxes can be tuned by appropriately choosing the Lorentz boost and a

[1]The beta beam concept was first proposed by Zucchelli to establish a facility for the search of leptonic CP violation [33]. For a discussion on the status of the feasibility of beta beam facilities, see, e.g., Ref. [34]. Note that Ref. [35] has proposed a method to reach high Q-value ion intensities, e.g., for ^{8}B and ^{8}Li, which is currently being investigated.

[2]Obviously, even larger ion boosts, around 10 or more, would be of interest. The numbers of 2–7 quoted in the available literature on low-energy beta beams was figured out to keep, in particular, the storage ring of small size.

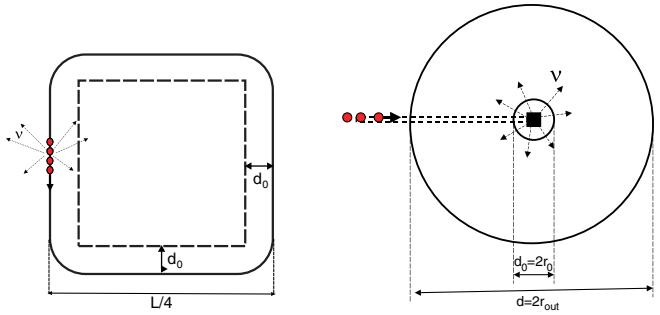

FIG. 1 (color online). Two possible scenarios to produce low-energy neutrinos from radioactive ions at a Lorentz boost of 1. Left figure: The radioactive ions decay while circulating in a storage ring. The neutrino detector is installed close to the ring. Right figure: The radioactive ions are injected into a cavity inside a spherical detector.

high/low Q-value ion. In the case where the ions are not boosted ($\gamma \approx 1$), storing the ions in a small storage ring is a possibility as well. An example is furnished by the storage ring facility currently proposed at HIE-ISOLDE at CERN [48]. While for this specific storage ring the number of stored ions is limited, one can imagine the establishment of a small ring at one of the future intense radioactive ion beam facilities, such as the European EURISOL [49] or the U.S. Facility for Rare Isotope Beams.

The second scenario to produce low-energy neutrinos consists in injecting the ions into a target placed inside the detector. It turns out that, as long as radioactive ions are slow (i.e., not accelerated to Lorentz-boost values above 1), such a scenario is much more efficient than the storage ring case. This is due to a geometrical effect, since only part of the produced (anti)neutrino flux—and not the total flux—traverses the detector if the ions are stored in a storage ring. The average neutrino flux at the detector is further reduced compared to the injection inside the detector case, if the detector cannot be located very close to the storage ring due to the background shielding and other necessary instrumentation.

In the rest frame, the beta decay of a nucleus produces the following (anti)neutrino flux as a function of neutrino energy:

$$\mathcal{N}(E_\nu) = f^{-1} E_\nu^2 E_e \sqrt{E_e^2 - m_e^2} F(Z, E_e) \Theta(E_e - m_e), \quad (1)$$

where f can be deduced from the measured $ft_{1/2}$ value. The quantities appearing in the above expression are the emitted lepton (electron or positron) energy $E_e = Q - E_\nu$ and the Fermi function $F(Z, E_e)$, which accounts for the Coulomb modification of the spectrum, with Z being the ion nuclear charge.

We consider that radioactive ions are produced and injected into a target with an intensity of I ions per second. This target is installed inside a cavity located at the center of a spherical detector. The corresponding (anti)neutrino flux at a distance r from the target is

$$\phi(E_\nu, r) = I \frac{\mathcal{N}(E_\nu)}{4\pi r^2}. \quad (2)$$

The neutrino event rate detected on a spherical surface segment of width dr, located at a distance r from the center of the detector, is given by

$$\frac{dN_i}{dt dE_\nu} = \phi(E_\nu, r) \sigma_i(E_\nu) \frac{n_i N_A \rho}{M_{\rm mol}} 4\pi r^2 dr. \quad (3)$$

Here $\sigma_i(E_\nu)$ is the neutrino capture cross section on the target material i, $M_{\rm mol}$ is the average molar mass of the detector material, n_i is the average number of nuclei of type i per mole of the detector material, and ρ is its density.

B. A coherent neutrino-nucleus scattering measurement

The measurement of coherent neutrino-nucleus scattering constitutes a precision test of the Standard Model, including the possibility of probing the weak nuclear charge as well as various deviations from the SM predictions, due to new physics above the weak scale or the presence of sterile neutrinos [28]. Coherent neutrino-nucleus scattering is also important in the astrophysical context, e.g., for core-collapse supernova physics.

Several proposals have been made to perform such a measurement, particularly near spallation sources [50,51]. Here we consider a setup as shown in Fig. 1 (right). The cross section for electron neutrino (or antineutrino) coherent scattering on a nucleus is given by [52,53]

$$\frac{d\sigma}{dT} = \frac{G_F^2}{4\pi} Q_W^2 M \left(1 - \frac{MT}{2E_\nu^2}\right) F(2MT)^2. \quad (4)$$

Here G_F is the Fermi constant, M is the nuclear mass, T the nuclear recoil energy, F the ground state elastic form factor, and

$$Q_W = N - (1 - 4\sin^2\theta_W) Z \quad (5)$$

the weak nuclear charge, with N the number of neutrons, Z the number of protons, and θ_W the weak mixing angle. For neutrino energies below 50 MeV, the momentum transfer is small and the form factor is close to unity, $F \sim 1$. For the measurement of neutrino-nucleus coherent scattering, different types of liquids are being discussed (see, e.g., Ref. [50]). Here we take liquid neon as an example.

C. A 3 + 1 sterile neutrino oscillation experiment

In the present work we consider a sterile neutrino search within the 3 + 1 framework, with three active neutrinos and one additional sterile neutrino. Besides the usual parameters of the Maki-Nakagawa-Sakata-Pontecorvo matrix, in this case the oscillation formula depends upon the neutrino mixing angle $\theta_{\rm new}$ and $\Delta m^2_{\rm new}$, considered to be much larger than $\Delta m^2_{31} \simeq 2.4 \times 10^{-3}$ eV^2. Implementing more complex scenarios with extra neutrinos is straightforward. The electron neutrino survival probability for $P_{ee}(E_\nu, r)$ is given by Ref. [54]:

$$P_{ee}(E_\nu, r) = 1 - \cos^4\theta_{\rm new}\sin^2(2\theta_{13})\sin^2\left(\frac{\Delta m^2_{31} r}{4E_\nu}\right) - \sin^2(2\theta_{\rm new})\sin^2\left(\frac{\Delta m^2_{\rm new} r}{4E_\nu}\right), \quad (6)$$

where a baseline of $L < 2$ km and neutrino energies $E_\nu > 2$ MeV are assumed. Equations (1)–(3) are used to determine the unoscillated number of events, while Eq. (3) has to be multiplied by the neutrino survival probability P_{ee} [Eq. (6)] in order to determine the number of oscillated events.

1. Statistical analysis and backgrounds

We present sensitivity plots obtained with the following procedure. We deal with systematic uncertainties inherent to the experimental setup by implementing the systematics directly into the statistical analysis by the use of the pull approach (see, for instance, Refs. [55,56]). Unless otherwise stated, we bin our data in energy as well as in R intervals of equal spacing, R being the distance from the center of the detector, with the χ^2 function being defined as

$$\chi^2 = \min_{\xi,\bar{\lambda}}\left[2\left(\sum_{ij} N^t_{ij} - n^f_{ij} - n^f_{ij}\ln\frac{N^t_{ij}}{n^f_{ij}}\right) + \xi^2\right], \quad (7)$$

where the sum runs over energy and R bins. As is customary in this type of analysis, a superscript t is used to denote the predicted number of events N^t_{ij}, while a superscript f is employed to denote the number of events obtained from the fitting to the simulated data, n^f_{ij}. The systematic error is indicated by π. It enters the analysis through the following definition:

$$N^t_{ij} = n^t_{ij} \times (1 + \pi\xi). \quad (8)$$

The respective true and fitted number of events, n^t_{ij} and n^f_{ij}, are functions of their corresponding oscillating parameters, but nonetheless the marginalization in Eq. (7) is performed over the subset of fitted parameters $\bar{\lambda}$ not held fixed during the fitting, as well as over the "pull" ξ.

The issue of background levels is an important one. First of all, we would like to stress that for the spherical detector setup (Fig. 1, right) we will not have sizeable beam-[3] or implantation-related backgrounds, since the ions implanted on the target are essentially at rest.[4] From previous experience with reactor experiments, the primary sources are environmental and geoneutrino backgrounds, which one could deal with in a relatively simple fashion by implementing an energy threshold around 4 MeV in the neutrino energy. The real problem is created by atmospheric muons, since one gets backgrounds via their high-energy neutrons or their spallation leftovers (^{9}Li). In order to reduce this kind of background signal to a tolerable level, one needs a detector design similar to that of, for instance, Daya Bay [57], where in addition to a rock overburden of at least 98 m (or 260 mwe), a 20 ton liquid target must be surrounded by a 20 ton gamma catcher and 40 tons of buffer volume. Under these conditions, the noise levels can be reduced to 6 events per ton per year. Therefore, to achieve such a low background event rate for the measurement under consideration here, it is necessary to locate the experiment well underground and surround the detector with appropriate shielding. In our calculations, we assume that this can be done, and we take as a reference value for the background 6 events per ton per year.

III. NUMERICAL RESULTS

To produce low-energy neutrinos, β^+ and β^- decaying ions can be considered as electron neutrino and antineutrino emitters, respectively.[5] The choice of the ions depends on the achievable intensities, the half-lives, and the Q values. Obviously the half-lives should lie in an appropriate range between short and long to make experiments feasible, so typically half-lives in the 1 s range seem to be a good choice. On the other hand, high Q values help by increasing the total number of events as well as improving the signal-to-background ratio.

Table I shows the candidate ions that we have been considering here as typical examples. Note that there exist a number of other promising radioactive ions, such as, e.g., ^{8}He or ^{12}N [59]. As far as ^{8}Li and ^{8}B are concerned, they decay mainly into a broad ^{8}Be $J^\pi = 2^+$ excited state at 3.03 MeV, therefore having Q values centered at 13.1 MeV and 15.1 MeV, respectively. Nevertheless, due to the broadness of the final state, the neutrino spectrum is extended well above the energy associated with the centered Q value. To evaluate qualitatively this effect, we present results for two decay modes[6]: i) 100% branching ratio to the ^{8}Be ground state; ii) 100% branching ratio to a narrow excited state at 3.03 MeV. In a real experiment, the actual results will fall in between these two "extreme" cases.

For the ion intensity, we assume 10^{13} ions per second. Instead of taking this parameter as a tunable number (as is sometimes done in the literature), here we consider values

[3]Note that for the storage ring configuration (Fig. 1, left) some background might be induced by the daughter nuclei colliding with the storage ring. Such a background can in principle be suppressed by putting an appropriate shielding around the storage ring.

[4]Note that the situation here is very different from the one where the ions are boosted at high γ. In this case there is again no beam-related background (a known advantage of the beta-beam concept), while there is radioactivity induced in the storage ring, arising, e.g., from collisions of the stable daughter nuclei on the ring. In this case a shielding is necessary to suppress the related backgrounds, and this has been considered in the previous literature on low-energy beta beams with γ larger than 1.

[5]Note that electron-capture neutrino beams have been considered in Ref. [58].

[6]Note that an accurate neutrino spectrum might be obtained by considering the ^{8}Be final state continuum, taking into account the delayed α spectrum [60].

TABLE I. Beta-decay properties of the ions considered in our proposal: τ is the decay lifetime; $E_\nu^{\max}$ is the end-point energy.

Ion	Decay	Daughter (State)	τ (ms)	$E_\nu^{\max}$ (MeV)
$^6_2$He	β^-	$^6_3$Li$(1^+, 0)$	806.7	3.5078
$^8_3$Li	β^-	$^8_4$Be$(2^+, 0)$	838	13.103
$^8_3$Li	β^-	$^8_4$Be$(0^+, 0)$	838	16.003
$^8_5$B	β^+	$^8_4$Be$(2^+, 0)$	770	15.079
$^8_5$B	β^+	$^8_5$Be$(0^+, 0)$	770	17.979

that can in principle be achievable at next-generation radioactive ion beam facilities. The predictions we present are obtained by taking 1 year $= 10^7$ s and assuming 100% efficiency for the detectors.

A. Expected neutrino-nucleus coherent scattering events

The goal of this section is to show the number of events associated with neutrino-nucleus scattering using realistic radioactive ion beam intensities achievable at future facilities. For a coherent neutrino-nucleus scattering measurement, both electron neutrino (β^+) and antineutrino (β^-) emitters can be used. In particular, we have considered ^{8}Li and ^{8}B and their two decay modes (Table I), and both the spherical and storage ring setups of Fig. 1. For a given ion intensity in the storage ring setup, the number of events is lower by at least a factor of 6 because the average flux at the detector is reduced by the usual factor $(4\pi r^2)^{-1}$, with r being the distance from the source. Therefore, we have decided to present results on the event rates for the spherical setup only, since the numbers appear to be low already in this case.

We take a 1 ton spherical liquid neon detector, where the ions are injected inside a central cavity having a 20 cm radius (Fig. 1, right). While other target nuclei are obviously possible, liquid neon is taken as an example. We would like to emphasize that detailed background simulations have already been done, e.g., for the CLEAR experiment proposed at the SNS spallation source facility [50]. The shielding envisaged for such a detector has been shown to reduce backgrounds near spallation sources to a negligible level. We expect that a similar reduction can be reached by putting the detector underground and/or using appropriate shielding. However, reaching very low nuclear recoils is challenging due to background issues (see, for example, Figs. 10 and 11 of Ref. [50]) and technical features like light quenching (for a discussion, see, e.g., Ref. [61]). Although very optimistic, a sensitivity threshold of 10 keV will be assumed. A higher energy threshold choice can be an option in the kinds of proposals discussed here only if much higher ion intensities can be attained.

Table II presents the number of expected events associated with electron (anti)neutrino scattering on neon.

TABLE II. Coherent neutrino-nucleus scattering: The expected number of events for the two candidate ions considered with the setup of Fig. 1, right (here 1 year $= 10^7$ s). The maximal neutrino energy is denoted by $E_\nu^{\max}$, and the nuclear recoil detection threshold by $T_{\min}$. The results correspond to an intensity of 10^{13} ions/s.

Ion	Decay	Target	$E_\nu^{\max}$ (MeV)	$T_{\min}$ (keV)	Events/ton/year
$^8_3$Li	β^-	Ne	13.103	10	192
$^8_3$Li	β^-	Ne	16.003	10	1373
$^8_5$B	β^+	Ne	15.079	10	846
$^8_5$B	β^+	Ne	17.979	10	3047

Figure 2 presents our predictions for the number of events for the two candidate ions considered as a function of the minimum measurable nuclear recoil. We recall that there is a maximum nuclear recoil [see Eq. (4)] that in our case is 27 (18) keV and 35 (24) keV, taking ^{8}Li and ^{8}B for the decay to the ground (excited) state as neutrino sources, respectively. Note that it is straightforward to scale our rates (Table II) with the ion intensity collected at the center of the 4π detector, or to take into account effects such as light quenching. One can see the strong sensitivity of the results to the maximal neutrino energy depending on the Q value of the ions. One can see that, despite the fact that coherence enhances the cross section relative to other type of processes, the low-energy range covered by the neutrino flux in this work makes the number of events still rather small compared to the number attainable with, e.g., the Michel spectrum of decay-at-rest muons produced at spallation sources [50]. Note that when shielding requirements are taken into account, the 20 cm diameter of the target region will probably need to be enlarged. For both setups, the feasibility of such a measurement strongly depends upon the achievable ion intensities. Reaching challenging low nuclear recoils in the detector and reducing backgrounds clearly represent key issues.

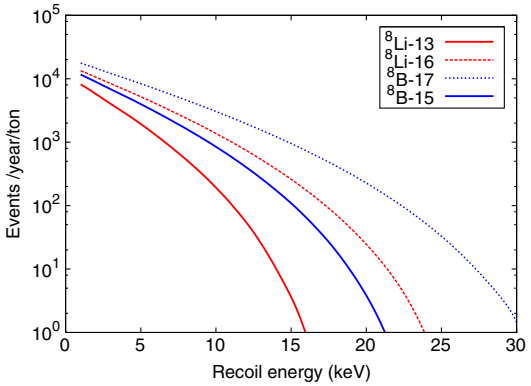

FIG. 2 (color online). Coherent neutrino-nucleus scattering: The expected number of events, as a function of the minimal nuclear recoil for the experimental setup of Figure 1 (right). The ^{8}B and ^{8}Li ion intensity is fixed at 10^{13} ions/s (here 1 year $= 10^7$ s).

B. Active-to-sterile neutrino oscillation exclusion plots

For the active-to-sterile neutrino oscillation search, we shall consider two types of β^- decaying ions (Table I). First, because of its very well-known aspects relating to its production and management, it is worth taking a look at the physics reach of a facility based on ^{6}He. Its low Q value yields a lower count, and as we will show, this hinders the potential of a setup exploiting this ion as opposed to one based upon a high Q-value ion choice. Our proposal for the search for sterile neutrinos is mainly based on the properties of ^{8}Li, for which we assume two extreme cases, indicated as ^{8}Li-16 MeV and ^{8}Li-13 MeV "ions."

Our choice of main setup has been dictated by an analysis of the performance of the two possible configurations shown in Fig. 1. In both cases, the considered detector is filled with a liquid scintillator.[7] The electron antineutrino detection channel is inverse beta decay: $\bar{\nu}_e + p \rightarrow n + e^+$. A good signal-to-background ratio can be obtained by the addition of gadolinium and the subsequent detection of the 8 MeV prompt gamma rays produced by the neutron capture.

For the case of the active-to-sterile neutrino oscillation hypothesis under consideration here, we have chosen to present the results of our simulations by means of exclusion plots based upon Eq. (7). The exclusion plots for the active-to-sterile oscillation parameter $\sin^2(2\theta_{\text{new}})$ are obtained by additionally fixing $\sin^2(2\theta_{13})$ to the best fit value of Ref. [62],[8] namely $\sin^2(2\theta_{13}) = 0.051$. Recently the Daya-Bay collaboration has measured the third neutrino mixing angle at 5.2σ to be $\sin^2 2\theta_{13} = 0.092 \pm 0.016(\text{stat}) \pm 0.005(\text{syst})$ [3]. We have checked that the plots presented here show no appreciable changes if the Daya-Bay value is used. The plots show the oscillation parameter space region where our setup is expected to be sensitive to the detection of active-to-sterile neutrino oscillations. In all our calculations, the considered running time of the experiment is 5 years. Unless contrarily stated, we fix the systematic error to $\pi = 1\%$ in all the analysis presented hereafter,[9] while we will show how our main results change if a larger systematic error is considered. We shall compare the sterile neutrino oscillation parameter regions that can be covered with our experimental setup to the allowed regions presented in the analysis of Ref. [21], based on reactor neutrino experimental data cumulated so far.

Figure 3 presents exclusion plots calculated from a statistical analysis of the data using total rates. The facility is based on ^{8}Li-13 MeV decaying ions. The aim of the figure is to compare the results obtained for the two experimental setups of Fig. 1. Note that for the specific case of the storage ring only, we assume an intensity of 10^{11} ions/s, having in mind a facility like HIE-ISOLDE (although the stored ion intensity is expected to be smaller [48]). Such an intensity should be attainable in a storage ring near the EURISOL facility [49]. For the setup geometry, following the TSR proposal for HIE-ISOLDE, we take a square storage ring with straight sections of 61.6 m length and a 1 kton cubic detector at the storage ring center.[10] (Such a geometry leaves 3 m of space between the detector and the storage ring straight sections [64,65].) Note that the number of expected events, and thus the exclusion plots, strongly depends on the setup geometry. For a large detector, as considered here, placing it in the center of the storage ring represents the optimal scenario. (If such a detector is located along one storage ring straight section, the event number is reduced by almost a factor of 4.) As expected, although the detector is only 20 tons, the performance obtained by sending the ions inside a 4π detector is superior to that of the storage ring setup[11] with respect to

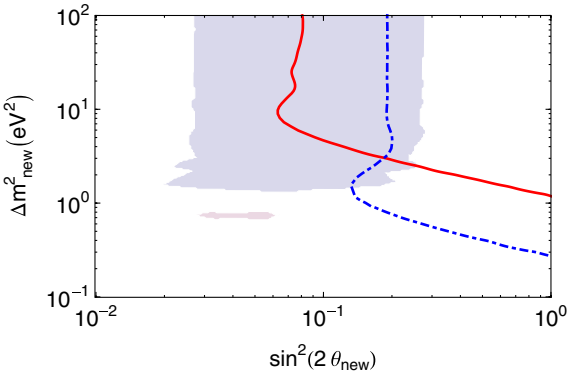

FIG. 3 (color online). Exclusion plots for the sterile neutrino mixing parameters from an analysis of the data including only total rates. The results are obtained by considering a 3 + 1 neutrino oscillation formalism. The contours shown are for a C.L. of 99% (2 d.o.f.). The two setups are those of Fig. 1. The solid (red) line corresponds to the 4π detector surrounding the source, while the dash-dotted (blue) line corresponds to the detector placed at the center of the square storage ring. The ion intensities are 10^{11} ions/s for the storage ring and 10^{13} ions/s for the spherical detector (see text). The source is composed of ^{8}Li ions decaying mainly to the first excited state of the daughter nucleus (maximal neutrino energy 13 MeV). In both cases a 5 yr running time is assumed. For comparison, the shaded region represents the 99% C.L. inclusion domain, given by the combination of reactor neutrino experiments and other sources (adapted from Fig. 8 of Ref. [21]).

[7]We take as an example $C_{16}H_{18}$ with a density of $\rho = 988\ \text{kg}/m^3$.

[8]Note that the exclusion curves change little if one fixes the third neutrino mixing angle to zero.

[9]Note that it is not our goal to discuss how lower systematic errors can be achieved in the actual experiment. For example, in Ref. [63], the authors discuss how this can be done in a short-baseline experiment at a neutrino factory.

[10]The detector base has a size of 9.4×9.4 m and a height of 11.3 m. Half of the detector is located below the storage ring, and half above.

[11]Note that this is also due to the higher ion intensity.

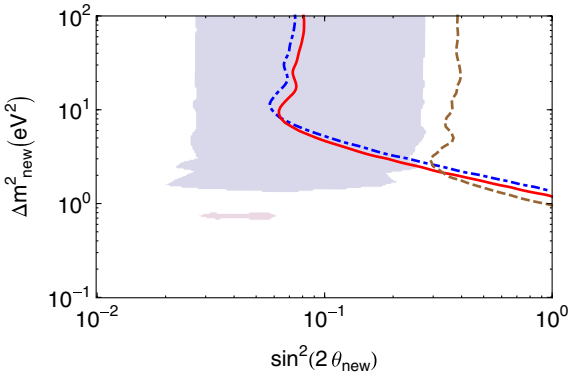

FIG. 4 (color online). Exclusion plots for the sterile neutrino mixing parameters from an analysis of the data including only total rates. The contours shown are for a C.L. of 99% (2 d.o.f.). The results correspond to choosing different ions: a source of ^{8}Li ions decaying mainly to the first excited state of the daughter nucleus (solid red line), ^{8}Li ions decaying mainly to the ground state of the daughter nucleus (dash-dotted blue line), or ^{6}He ions (dashed brown line). For comparison, the shaded region represents the 99% C.L. inclusion domain, given by the combination of reactor neutrino experiments and other sources (adapted from Fig. 8 of Ref. [21]).

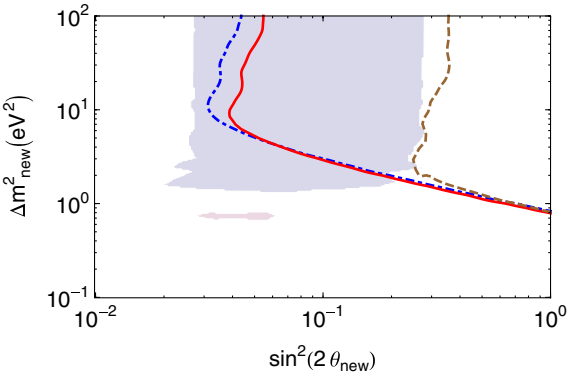

FIG. 5 (color online). Exclusion plots for the sterile neutrino mixing parameters, with binned analysis of the simulated data both in neutrino energy and in distance within the detector. The contours shown are for a C.L. of 99% (2 d.o.f.). The results correspond to choosing different ions: a source of ^{8}Li ions decaying mainly to the first excited state of the daughter nucleus (solid red line), ^{8}Li ions decaying mainly to the ground state of the daughter nucleus (dash-dotted blue line), or ^{6}He ions (dashed brown line). For comparison, the shaded region represents the 99% C.L. inclusion domain, given by the combination of reactor neutrino experiments and other sources (adapted from Fig. 8 of Ref. [21]).

coverage of the shaded region identified by the reactor anomaly. On the other hand, the storage ring setup has a better sensitivity to small Δm^2. In addition to the aforementioned geometric advantages, the spherical detector setup benefits from the fact that neutrino source is very close to the active detector material (we recall that the radius cavity is only 20 cm). From now on, all the results we present will correspond to the spherical detector setup.

Figures 4 and 5 show exclusion plots constructed from total rates, and from a spectral (binned) analysis of the simulated data, respectively. For the binned case, 8 energy bins and 8 R bins of equal size are considered. Note that, for the binned case, the corresponding background in the detector is scaled accordingly (it grows radially as R^2). Results for three ion sources are shown: the ^{8}Li-16 MeV, ^{8}Li-13 MeV, and ^{6}He cases. The low Q value of the helium ions clearly hinders the sensitivity of this setup, making it clearly inferior to the lithium ion source case. Notice the slight difference between the two ^{8}Li cases, which is only marginally enhanced for the binned case for large $\Delta m^2_{\rm new}(>7\ \rm eV^2)$. (Small) corrections from ions decaying to the ground state of the daughter nucleus are thus expected to be important only in the large $\Delta m^2_{\rm new}$ case. The results of Fig. 5 show the importance of appropriate binning.

For comparison, we have also included in these figures shaded regions corresponding to the 99% C.L. inclusion domains identified by the combination of data from the reactor neutrino experiments and other sources, as described in, and here adapted from, Fig. 8 of Ref. [21]. One can see that the proposal investigated here would allow us to cover most of the active-to-sterile oscillation parameter region. On the other hand, we recall that the presented exclusion curves have the following simple physical meaning: an actual measurement lying inside the curve (to the upper right of the curve) represents definite evidence in favor of the corresponding hypothesis; in our case, active neutrinos oscillating into sterile ones. In this manner, from Fig. 5 one sees that the shaded region is out of reach if one uses 10^{13} ^{6}He/s, whereas using

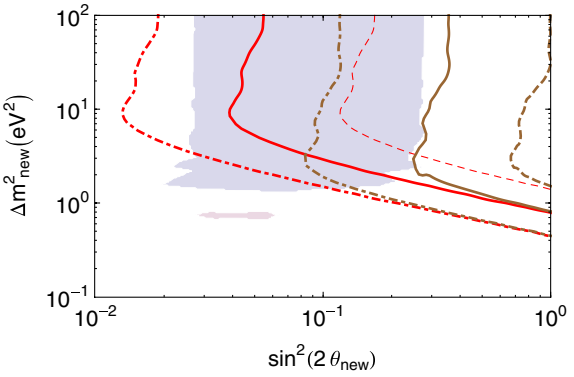

FIG. 6 (color online). Exclusion plots with binned analysis of the simulated data, obtained by varying the ion intensity: 10^{14} ions/s (dash-dotted), 10^{13} ions/s (solid), and 10^{12} ions/s (dashed). The red lines correspond to the source of ^{8}Li ions decaying mainly to the first excited state of the daughter nucleus (maximal neutrino energy 13 MeV), while the brown lines correspond to the source of ^{6}He ions. The contours shown are for a C.L. of 99% (2 d.o.f.). For comparison, the shaded region represents the 99% C.L. inclusion domain, given by the combination of reactor neutrino experiments and other sources (adapted from Fig. 8 of Ref. [21]).

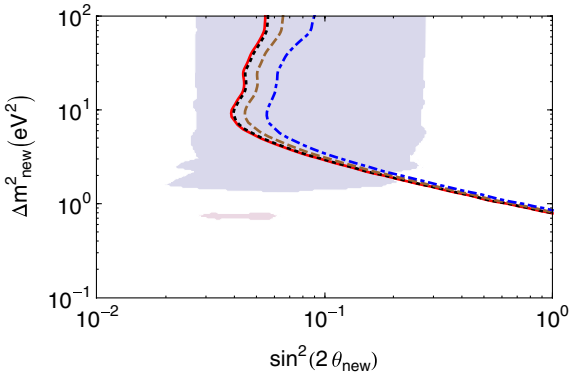

FIG. 7 (color online). Exclusion plots with binned analysis of the simulated data, obtained for 10^{13} ions/s with ^{8}Li ions decaying mainly to a 13 MeV excited state of the daughter nucleus. The figure shows the impact on the exclusion curves of different levels of systematic error, namely 1% (solid, red), 2% (dotted, black), 5% (dashed, brown), and 10% (dash-dotted, blue). The contours shown are for a C.L. of 99% (2 d.o.f.). For comparison, the shaded region represents the 99% C.L. inclusion domain, given by the combination of reactor neutrino experiments and other sources (adapted from Fig. 8 of Ref. [21]).

10^{13} ^{8}Li/s one can cover around 70%–75% of the currently allowed region.

We would like to discuss now the impact of the chosen ion intensities on the setup performance. Figure 6 shows how the exclusion plots (and the coverage of the allowed region) change when varying the ion intensity. In particular, the physics potential, relative to our main setup with 10^{13} ions/s, is seen to diminish (increase) by changing the intensity by 1 order of magnitude. This speaks of the high level of influence that achieving good ion production levels

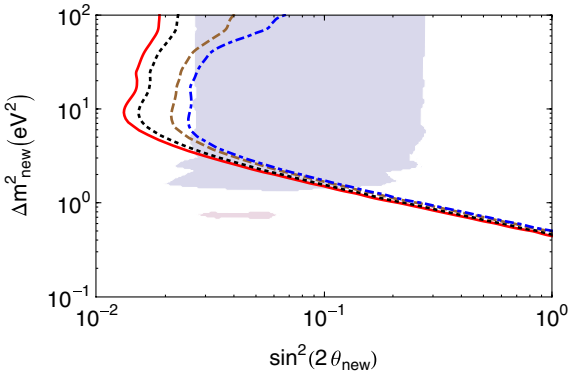

FIG. 8 (color online). Exclusion plots with binned analysis of the simulated data, obtained for 10^{14} ions/s with ^{8}Li ions decaying mainly to a 13 MeV excited state of the daughter nucleus. The figure shows the impact on the exclusion curves of different levels of systematic error, namely 1% (solid, red), 2% (dotted, black), 5% (dashed, brown), and 10% (dash-dotted, blue). The contours shown are for a C.L. of 99% (2 d.o.f.). For comparison the shaded region represents the 99% C.L. inclusion domain, given by the combination of reactor neutrino experiments and other sources (adapted from Fig. 8 of Ref. [21]).

near future radioactive ion beam facilities can have upon this type of experimental search. Production methods to reach high intensities for specific radioactive ions such as ^{6}He and ^{8}Li are being investigated (see e.g., Refs. [66,67]).

Finally, the sensitivity of the proposed experiment might depend upon the achieved systematic errors. To show their impact, we present exclusion curves based upon a binned analysis for sterile neutrino mixing parameters, for different levels of systematic errors. Figures 7 and 8 show the impact of 1%, 2%, 5%, and 10% systematic error on the exclusion curves for 10^{13} and 10^{14} ^{8}Li/s, respectively. One can see the important impact that reaching low systematic errors has, especially for a large Δm^2 and small mixing angle.

IV. CONCLUSIONS

Future intense radioactive ion beam facilities can offer a unique opportunity to perform searches for beyond the Standard Model physics, using low-energy neutrino fluxes from beta-decaying ions. Here we consider two configurations, where the ions are either stored in a storage ring or sent into a target inside a spherical detector, filled either with a noble liquid or with a scintillator (with the addition of gadolinium). Our results show that, as long as the ions are not boosted, the spherical geometry scenario gives better results than the storage ring one. We have presented predictions for the expected events associated with a coherent neutrino-nucleus scattering measurement. The realization of such an experiment heavily depends on the achievement of large ion intensities and reaching challenging low-energy nuclear recoils. The second option considered is a sterile neutrino search, that can be performed using electron antineutrino detection through inverse beta decay in a scintillator. We have presented exclusion plots obtained from total rates and from analysis including spectral information (with binning in neutrino energy and in distance within the detector) of the simulated data. In particular, the binned analysis gives interesting results for ion intensities achievable at future radioactive ion beam facilities, like the EURISOL facility. Clearly the ion intensities achievable at such facilities are lower than the MCi radioactive source considered in proposals like the one in Ref. [26]. However, radioactive ion beam facilities offer the possibility to dispose of radioactive ions with different Q values, allowing us to cover different regions of the oscillation parameters. With our spherical setup, one can probe large squared-mass differences and rather small mixing angle values, associated with one sterile neutrino, in the 3 + 1 oscillation framework. In particular, with the kind of setup we consider here, one could confirm/rule out the sterile neutrino hypothesis as a possible explanation of the currently debated reactor neutrino anomaly, and cover most of the corresponding parameter space region.

ACKNOWLEDGMENTS

We are grateful to Guido Drexlin for important discussions on background issues, for his encouragement in pursuing this

project, and for his careful reading of this manuscript. We would like to thank Klaus Blaum and Manfred Grieser for providing us with the TSR characteristics, Kate Scholberg for information concerning backgrounds and the CLEAR proposal, Thierry Stora for the ion intensities at HIE-ISOLDE as well as Michael Hass and Tsviki Hirsh for information on ^{8}Li production, and Mauro Mezzetto for useful discussions on sensitivity issues. C. E.-H. acknowledges the support by IPN Orsay, and in part by the Grant Generalitat Valenciana VALi + d, PROMETEO Grant No. 2008/004, and FPA Grant No. 2008/02878 of Spanish Ministry MICINN.

Note added.—After completing this manuscript, the authors have discovered Ref. [31], which presents an overlap with the present work.

[1] K. Abe *et al.* (T2K Collaboration), Phys. Rev. Lett. **107**, 041801 (2011).
[2] Y. Abe *et al.* (DOUBLE-CHOOZ Collaboration), Phys. Rev. Lett. **108**, 131801 (2012).
[3] F. P. An *et al.* (Daya-Bay Collaboration), Phys. Rev. Lett. **108**, 171803 (2012).
[4] J. K. Ahn *et al.* (RENO Collaboration), Phys. Rev. Lett. **108**, 191802 (2012).
[5] A. B. Balantekin and D. Yilmaz, J. Phys. G **35**, 075007 (2008).
[6] G. L. Fogli, E. Lisi, A. Marrone, A. Palazzo, and A. M. Rotunno, arXiv:0905.3549.
[7] P. Huber, M. Lindner, T. Schwetz, and W. Winter, J. High Energy Phys. 11 (2009) 044.
[8] C. Volpe, J. Phys. G **34**, R1 (2007).
[9] J. Alonso, F. T. Avignone, W. A. Barletta, R. Barlow, H. T. Baumgartner, A. Bernstein, E. Blucher, L. Bugel *et al.*, arXiv:1006.0260.
[10] J. Bonn (KATRIN Collaboration), Prog. Part. Nucl. Phys. **64**, 285 (2010).
[11] A. B. Balantekin, J. Gava, and C. Volpe, Phys. Lett. B **662**, 396 (2008).
[12] J. Gava and C. Volpe, Phys. Rev. D **78**, 083007 (2008).
[13] J. Gava and C. Volpe, Nucl. Phys. **B837**, 50 (2010).
[14] G. C. McLaughlin, J. M. Fetter, A. B. Balantekin, and G. M. Fuller, Phys. Rev. C **59**, 2873 (1999).
[15] K. Abazajian, N. F. Bell, G. M. Fuller, and Y. Y. Y. Wong, Phys. Rev. D **72**, 063004 (2005).
[16] J. Hamann, S. Hannestad, G. G. Raffelt, and Y. Y. Y. Wong, J. Cosmol. Astropart. Phys. 09 (2011) 034.
[17] A. A. Aguilar-Arevalo *et al.* (MiniBooNE Collaboration), Phys. Rev. Lett. **102**, 101802 (2009).
[18] C. Athanassopoulos *et al.* (LSND Collaboration), Phys. Rev. Lett. **77**, 3082 (1996).
[19] C. Athanassopoulos *et al.* (LSND Collaboration), Phys. Rev. Lett. **81**, 1774 (1998).
[20] B. Zeitnitz, B. Armbruster, M. Becker, A. Benen, G. Drexlin, V. Eberhard, K. Eitel, H. Gemmeke *et al.*, Prog. Part. Nucl. Phys. **40**, 169 (1998).
[21] G. Mention, M. Fechner, T. Lasserre, T. A. Mueller, D. Lhuillier, M. Cribier, and A. Letourneau, Phys. Rev. D **83**, 073006 (2011).
[22] T. A. Mueller, D. Lhuillier, M. Fallot, A. Letourneau, S. Cormon, M. Fechner, L. Giot, T. Lasserre *et al.*, Phys. Rev. C **83**, 054615 (2011).
[23] C. Giunti and M. Laveder, Phys. Rev. C **83**, 065504 (2011).
[24] C. Giunti and M. Laveder, Phys. Rev. D **84**, 073008 (2011).
[25] E. Akhmedov and T. Schwetz, J. High Energy Phys. 10 (2010) 115.
[26] M. Cribier, M. Fechner, T. Lasserre, A. Letourneau, D. Lhuillier, G. Mention, D. Franco, V. Kornoukhov, and S. Schönert, Phys. Rev. Lett. **107**, 201801 (2011).
[27] J. D. Vergados, Y. Giomataris, and Y. N. Novikov, Phys. Rev. D **85**, 033003 (2012).
[28] A. J. Anderson, J. M. Conrad, E. Figueroa-Feliciano, C. Ignarra, G. Karagiorgi, K. Scholberg, M. H. Shaevitz, and J. Spitz, Phys. Rev. D **86**, 013004 (2012).
[29] D. A. Dwyer, K. M. Heeger, B. R. Littlejohn, and P. Vogel, arXiv:1109.6036.
[30] O. Yasuda, J. High Energy Phys. 09 (2011) 036.
[31] S. K. Agarwalla and R. S. Raghavan, arXiv:1011.4509.
[32] C. Volpe, J. Phys. G **30**, L1 (2004).
[33] P. Zucchelli, Phys. Lett. B **532**, 166 (2002).
[34] E. Wildner, Acta Phys. Pol. B **41**, 1525 (2010).
[35] C. Rubbia, A. Ferrari, Y. Kadi, and V. Vlachoudis, Nucl. Instrum. Methods Phys. Res., Sect. A **568**, 475 (2006).
[36] J. Serreau and C. Volpe, Phys. Rev. C **70**, 055502 (2004).
[37] G. C. McLaughlin, Phys. Rev. C **70**, 045804 (2004).
[38] R. Lazauskas and C. Volpe, Nucl. Phys. **A792**, 219 (2007).
[39] A. R. Samana, F. Krmpotic, N. Paar, and C. A. Bertulani, Phys. Rev. C **83**, 024303 (2011).
[40] G. C. McLaughlin and C. Volpe, Phys. Lett. B **591**, 229 (2004).
[41] A. B. Balantekin, J. H. de Jesus, R. Lazauskas, and C. Volpe, Phys. Rev. D **73**, 073011 (2006).
[42] A. B. Balantekin, J. H. de Jesus, and C. Volpe, Phys. Lett. B **634**, 180 (2006).
[43] J. Barranco, O. G. Miranda, and T. I. Rashba, Phys. Rev. D **76**, 073008 (2007).
[44] A. Bueno, M. C. Carmona, J. Lozano, and S. Navas, Phys. Rev. D **74**, 033010 (2006).
[45] S. K. Agarwalla, P. Huber, and J. M. Link, J. High Energy Phys. 01 (2010) 071.
[46] N. Jachowicz and G. C. McLaughlin, Phys. Rev. Lett. **96**, 172301 (2006).
[47] C. Volpe, J. Phys. G **31**, 903 (2005).
[48] See M. Grieser *et al.*, CERN Report No. INTC-2012-027; Report No. INTC-O-014, http://cdsweb.cern.ch/record/1411615.
[49] http://www.ganil-spiral2.eu/eurisol.
[50] K. Scholberg *et al.*, arXiv:0910.1989.
[51] J. D. Vergados, F. T. Avignone, and I. Giomataris, Phys. Rev. D **79**, 113001 (2009).

[52] D. Z. Freedman, Phys. Rev. D **9**, 1389 (1974).
[53] C. J. Horowitz, K. J. Coakley, and D. N. McKinsey, Phys. Rev. D **68**, 023005 (2003).
[54] A. de Gouvea and T. Wytock, Phys. Rev. D **79**, 073005 (2009).
[55] P. Huber, M. Lindner, and W. Winter, Nucl. Phys. **B645**, 3 (2002).
[56] G. L. Fogli, E. Lisi, A. Marrone, D. Montanino, A. Palazzo, and A. M. Rotunno, Phys. Rev. D **67**, 073002 (2003).
[57] X. Guo *et al.* (Daya-Bay Collaboration), arXiv:hep-ex/0701029.
[58] J. Bernabeu, J. Burguet-Castell, C. Espinoza, and M. Lindroos, J. High Energy Phys. 12 (2005) 014.
[59] B. Autin *et al.*, J. Phys. G **29**, 1785 (2003).
[60] M. Bhattacharya and E. G. Adelberger, Phys. Rev. C **65**, 055502 (2002).
[61] D. M. Mei, Z. B. Yin, L. C. Stonehill, and A. Hime, Astropart. Phys. **30**, 12 (2008).
[62] T. Schwetz, M. Tortola, and J. W. F. Valle, New J. Phys. **13**, 109401 (2011).
[63] C. Giunti, M. Laveder, and W. Winter, Phys. Rev. D **80**, 073005 (2009).
[64] M. Grieser (private communication).
[65] M. Grieser, Y. A. Litvinov, R. Raabe, K. Blaum, Y. Blumenfeld, P. A. Butler, F. Wenander, P. J. Woods *et al.*, Eur. Phys. J. Special Topics **207**, 1 (2012).
[66] M. Hass, D. Berkovits, T. Y. Hirsh, V. Kumar, M. Lewitowicz, F. de Oliveira, and S. Veintraub, J. Phys. G **35**, 014042 (2008).
[67] T. Stora, E. Noah, R. Hodak, T. Y. Hirsh, M. Hass, V. Kumar, K. Singh, and S. Vaintraub *et al.*, Europhys. Lett. **98**, 32001 (2012).